Generation of continuous-wave broadband entangled beams using periodically poled lithium niobate waveguides

Ken-ichiro Yoshino, Takao Aoki, and Akira Furusawa[a)]
Department of Applied Physics, School of Engineering, The University of Tokyo, 7-3-1 Hongo, Bunkyo-ku, Tokyo 113-8656, Japan and CREST, Japan Science and Technology Agency, 1-9-9 Yaesu, Chuoh-ku, Tokyo 103-0028, Japan

(Received 20 September 2006; accepted 1 January 2007; published online 25 January 2007)

Continuous-wave light beams with broadband quantum entanglement are created with two independent squeezed light beams generated by two periodically poled lithium niobate waveguides and a symmentric beam splitter. The quantum entanglement is confirmed with a sufficient criterion $\Delta^2_{A,B}=\langle[\Delta(\hat{x}_A-\hat{x}_B)]^2\rangle+\langle[\Delta(\hat{p}_A+\hat{p}_B)]^2\rangle<1$ and the observed $\Delta^2_{A,B}$ is 0.75 over the bandwidth of 30 MHz. Although the bandwidth is limited by that of the detector so far, it would be broadened up to 10 THz which would be only limited by the bandwidth of phase matching for the second-order nonlinear process. © *2007 American Institute of Physics*. [DOI: 10.1063/1.2437057]

Quantum information processing is intensively studied as next-generation information processing. There are two types of streams for quantum information processing: quantum bit[1] (qubit) and continuous variables (CVs).[2] CV quantum information processing is relatively easy to be implemented in experiments since it can be based on highly efficient homodyne detection instead of photon counting, which suffers from low detection efficiency. The heart of CV quantum information processing is quantum entanglement which was originally proposed by Einstein *et al.* in 1935.[3]

In quantum optics, the quantum entanglement is embodied as a two-mode squeezed vacuum[4–6] where quadrature field modes are correlated in two light beams (entangled beams). There are some quantum optical schemes to create them; a continuous-wave (cw) light scheme[4,5] and a pulsed light scheme.[6] For quantum information processing, the cw scheme might have some advantage because one can use the well-matured cw scheme of quantum teleportation,[7,8] where complicated interferometers are constructed by taking advantage of the long coherence length of cw light. Because of this fact, cw entangled beams can be easily used for various quantum information processing protocols. Thus it is important to create cw entangled beams.

So far cw entangled beams are generated from optical parametric process with optical-cavity enhancement. The usage of cavities limits the bandwidth of quantum entanglement within the cavity bandwidth. For broadband CV quantum information processing, one has to have the other enhancement mechanism of the parametric process. One of the best ways for it is the usage of a waveguide.[9–11] Since a waveguide can concentrate and keep large power density of a pump beam throughout the interaction length, it does not have any limit of the bandwidth except for that of phase matching.

In this letter, we demonstrate experimental creation of cw entangled beams with two independent squeezed light beams generated by two periodically poled lithium niobate (PPLN) waveguides and a symmetric beam splitter. We observe quantum entanglement over the bandwidth of 30 MHz. Although the bandwidth is limited by that of the detector so far, it would be broadened up to 10 THz which would be only limited by the bandwidth of phase matching for the second-order nonlinear process.

Now let us briefly explain our notation of quantum states including squeezed states and those of entangled beams, and then introduce how to evaluate the quality of entangled beams. In order to describe the evolution of quantum states of optical fields, we use the Heisenberg picture. We introduce quadrature-phase amplitude operators $\hat{x}$ and $\hat{p}$, corresponding to the real and imaginary parts of an optical field mode's annihilation operator $\hat{a}=\hat{x}+i\hat{p}$ (units free with $\hbar=1/2$, $[\hat{x},\hat{p}]=i/2$).

Sidebands of squeezed light beams ($\hat{a}_1$, $\hat{a}_2$) in this experiment can be expressed as

$$\hat{a}_1 = e^r\hat{x}_1^{(0)} + ie^{-r}\hat{p}_1^{(0)},$$

$$\hat{a}_2 = e^{-r}\hat{x}_2^{(0)} + ie^{r}\hat{p}_2^{(0)}, \tag{1}$$

where $\hat{x}_1^{(0)}$, $\hat{p}_1^{(0)}$, $\hat{x}_2^{(0)}$, and $\hat{p}_2^{(0)}$ are quadrature-phase amplitudes of initial vacuum states and r is a squeezing parameter.

By combining these two modes with a symmetric beam splitter, the two output beams become entangled beams. Output modes ($\hat{a}_A$, $\hat{a}_B$) from the symmetric beam splitter can be expressed as

$$\hat{a}_A = \hat{a}_1 + \hat{a}_2,$$

$$\hat{a}_B = \hat{a}_1 - \hat{a}_2. \tag{2}$$

Thus the output modes ($\hat{a}_A=\hat{x}_A+i\hat{p}_A$, $\hat{a}_B=\hat{x}_B+i\hat{p}_B$) show the following correlations:

$$\hat{x}_A - \hat{x}_B = \sqrt{2}e^{-r}\hat{x}_2^{(0)},$$

$$\hat{p}_A + \hat{p}_B = \sqrt{2}e^{-r}\hat{p}_1^{(0)}. \tag{3}$$

We check the entanglement by using the inseparability criterion proposed by Duan *et al.*[12] and Simon.[13] We define $\Delta^2_{A,B}$ described as follows:

$$\Delta^2_{A,B} = \langle[\Delta(\hat{x}_A - \hat{x}_B)]^2\rangle + \langle[\Delta(\hat{p}_A + \hat{p}_B)]^2\rangle. \tag{4}$$

When $\Delta^2_{A,B}$ is less than unity, it is proven that these two beams are entangled. In the present experiment we check $\Delta^2_{A,B}<1$ over a wide frequency range.

[a)]Electronic mail: akiraf@ap.t.u-tokyo.ac.jp

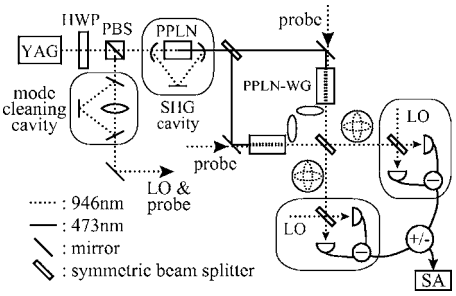

FIG. 1. Experimental setup for generation of broadband entangled beams. HWP: half wave plate, PBS: polarization beam splitter, PPLN-WG: periodically poled lithium niobate waveguide, LO: local oscillator, SA: spectrum analyzer. The ellipses indicate the squeezed quadratures of each beam.

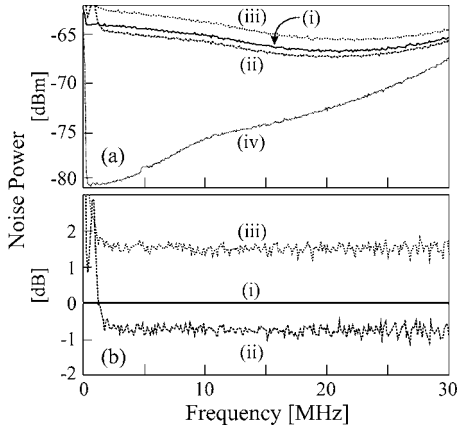

FIG. 2. Noise measurement results on a squeezed light beam generated by a PPLN waveguide. These are recorded by one of the homodyne detectors after passing through a symmetric beam splitter. (a) is the raw results including the detector's noise. (b) is the results after compensation. The vacuum noise level is normalized to 0 dB and the effect of the detector's noise is subtracted. In each figure, traces (i), (ii), and (iii) show the noise levels of a vacuum, squeezed quadrature, and antisqueezed quadrature respectively. In Fig. (a), trace (iv) represents the detector's noise. The LO power is set to 3.5 mW, resolution bandwidth (RBW) is 100 kHz, and video bandwidth (VBW) is 100 Hz. All traces are averaged ten times.

Our experimental setup is shown in Fig. 1. Output of a Nd:YAG (yttrium aluminum garnet) laser at 946 nm (Innolight Mephisto QTL, output power of ~500 mW) is divided into two beams by a half wave plate and a polarization beam splitter. About 10% of the total power goes to a mode cleaning cavity (MCC). The rest 90% is used for second-harmonic generation (SHG) to pump PPLN waveguides (NGK Corp., Japan) to generate squeezed light beams. The shape of cross section of the PPLN waveguides is a trapezoid whose base and height are about 5 and 3.5 μm, respectively. The length of the waveguide is 12 mm. The squeezed light beams and the entangled beams are measured with homodyne detectors which have Si photodiodes (Hamamatsu S3590-06, antireflective coated at 946 nm) with quantum efficiency of 99.4% at 946 nm.

The MCC prepares local oscillators (LOs) for homodyne detection. The MCC acts as a spatial filter, so we can obtain a nearly ideal Gaussian fundamental mode. In practice, although the spatial modes of the waveguides are somewhat different from Gaussian fundamental modes, we assume they are similar to each other. Moreover, we can obtain very stable output power from the MCC because the cavity length is so controlled that the output power stays to be constant, instead of locking to a peak of cavity transmission. As the result, we can reduce the drift of the LO powers within 0.2 dB.

About 90% of the output of the Nd:YAG laser is frequency doubled in an external cavity with a bulk crystal of PPLN inside. At the early stage of the experiment, we tried to use a PPLN waveguide for SHG, but the coupling efficiency of fundamental wave (946 nm) to the waveguide was very low (about 65% at most), and actual SHG efficiency of the waveguide was worse than that of the external cavity with a bulk PPLN crystal inside. Therefore we chose a bulk PPLN crystal for SHG, and it can generate 190 mW second harmonic at 473 nm from 430 mW of fundamental power. The SHG output is divided into two beams by a symmetric beam splitter to pump the PPLN waveguides. About 90 mW second harmonic at 473 nm goes to each PPLN waveguide, and about 30 mW can be coupled. Broadband squeezed states are generated by parametric amplification process in the waveguides, which is the reverse process of SHG.

By using phase matching condition of a PPLN waveguide, we can calculate the phase matching linewidth.[14,15] According to the calculation, the linewidth of the squeezed states generated by the PPLN waveguides is about 30 nm, and it corresponds to about 10 THz bandwidth in the frequency domain. This means the observed bandwidth of squeezed states from the PPLN waveguides is only limited by that of the homodyne detectors (~30 MHz).

The entangled beams are created by combining two squeezed light beams from each PPLN waveguide at a symmetric beam splitter with orthogonal phases ($\pi/2$ phase shift) to each other, as shown by the ellipses in Fig. 1. For this purpose, we inject weak coherent beams from the MCC to the waveguides, which are denoted as "probes" in Fig. 1. The phases of the coherent beams are locked to the squeezing quadratures. With the interference fringe between the coherent beams at the symmetric beam splitter, we lock the relative phase of the squeezed light beams. Furthermore, the coherent beams have modulation sidebands at 70 and 80 kHz, respectively, and they are used for locking the LO phases at the homodyne detectors.

The output beams of the symmetric beam splitter are distributed to two homodyne detectors, and noise powers of the beams are measured in each quadrature phase by a spectrum analyzer (Agilent E4401). Spatial mode matching efficiencies between the coherent beams and LOs, which represent those between squeezed light beams from the waveguides and LOs, are about 0.94 and 0.86, respectively. These relatively low values are due to the deviation of the spatial modes of the waveguides from Gaussian fundamental modes. The LO powers at each homodyne detector are set to be 3.5 mW, and they are stabilized by the MCC, as mentioned before.

First, we measure a squeezed light beam from one PPLN waveguide at one of the homodyne detectors. Here, the other squeezed light beam is blocked just after the other PPLN waveguide. Figure 2 shows the results obtained by a spectrum analyzer. Since the squeezed light is measured after passing through the symmetric beam splitter, it suffers from 50% losses.

Figure 2(a) shows raw data on noise powers of a vacuum, the squeezed quadrature, the anti-squeezed quadrature, and the homodyne detector itself. In Fig. 2(b), the noise level of the vacuum state is normalized to 0 dB, and the detector noises are subtracted. The noise level of the

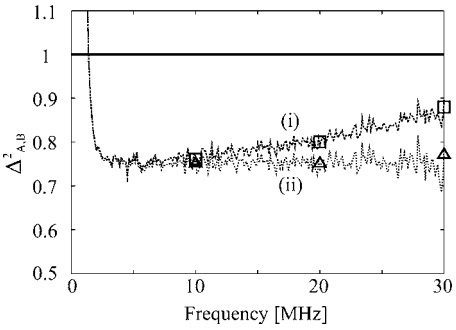

FIG. 3. Results on the inseparability criterion, $\Delta^2_{A,B}=\langle[\Delta(\hat{x}_A-\hat{x}_B)]^2\rangle+\langle[\Delta(\hat{p}_A+\hat{p}_B)]^2\rangle$. (i) and (ii) represent $\Delta^2_{A,B}$ at 100 kHz RBW before and after subtracting the effects of detector's noise, respectively. Squares and triangles are results at 5 MHz RBW before and after noise compensation.

squeezed light is about −0.76 dB compared to that of the vacuum, and it is almost flat up to 30 MHz. If the squeezed light would be measured directly, that is, without the symmetric beam splitter, the squeezing level would be calculated as −1.7 dB.

Next, we proceed to the measurement of quantum entanglement and unblock the other squeezed light beam. We set the LO phases for homodyne detection so as to obtain x or p quadrature component of each beam. The signals from the homodyne detectors are subtracted or summed electronically and the variance is measured by a spectrum analyzer in a wide spectral range. In order to get the value of $\langle[\Delta(\hat{x}_A-\hat{x}_B)]^2\rangle$, we set the LO phases at x quadrature, and for $\langle[\Delta(\hat{p}_A+\hat{p}_B)]^2\rangle$ we set them at p quadrature. Then $\Delta^2_{A,B}$ is calculated with Eq. (4).

The experimental results on $\Delta^2_{A,B}$ are shown in Fig. 3. We can see that $\Delta^2_{A,B}$ is below unity up to 30 MHz, which is the detector bandwidth. Furthermore, if the detector noises are subtracted, $\Delta^2_{A,B}$ is nearly flat at about 0.75 over the whole spectral range [curve (ii)].

Up to here, we took a narrowband spectral filter of the spectrum analyzer [resolution bandwidth (RBW)=100 kHz] in order to see the frequency characteristics in detail. However, since our present goal is to broaden the bandwidth of quantum entanglement, we measure $\Delta^2_{A,B}$ with a broadband filter (RBW=5 MHz), which is the broadest filter of the spectrum analyzer. The results are plotted in Fig. 3. Even when the RBW is broadened, we can still see almost the same value of $\Delta^2_{A,B}$. It indicates that broadband entangled beams are generated successfully. Note that although we use the weak coherent beams to lock the phases of squeezed light beams and LOs in the present experiments, we can remove them by using the "sample and hold" technique.[16]

In conclusion, cw entangled beams are created with two independent squeezed light beams generated by two PPLN waveguides and a symmetric beam splitter. The quantum entanglement is confirmed with a sufficient criterion $\Delta^2_{A,B}=\langle[\Delta(\hat{x}_A-\hat{x}_B)]^2\rangle+\langle[\Delta(\hat{p}_A+\hat{p}_B)]^2\rangle<1$ and the observed $\Delta^2_{A,B}$ is 0.75 over the bandwidth of 30 MHz. Although the bandwidth is limited by that of the detector so far, it would be broadened up to 10 THz, which would be only limited by the bandwidth of phase matching for the second-order nonlinear process.

[1] M. A. Nielsen and I. L. Chuang, *Quantum Computation and Quantum Information* (Cambridge University Press, Cambridge, 2000), 13.
[2] S. L. Braunstein and P. van Loock, Rev. Mod. Phys. **77**, 513 (2005).
[3] A. Einstein, B. Podolsky, and N. Rosen, Phys. Rev. **47**, 777 (1935).
[4] M. D. Reid, Phys. Rev. A **40**, 913 (1989).
[5] Z. Y. Ou, S. F. Pereira, H. J. Kimble, and K. C. Peng, Phys. Rev. Lett. **68**, 3663 (1992).
[6] J. Wenger, A. Ourjoumtsev, R. Tualle-Brouri, and P. Grangier, Eur. Phys. J. D **32**, 391 (2005).
[7] A. Furusawa, J. L. Sørensen, S. L. Braunstein, C. A. Fuchs, H. J. Kimble, and E. S. Polzik, Science **282**, 706 (1998).
[8] N. Takei, H. Yonezawa, T. Aoki, and A. Furusawa, Phys. Rev. Lett. **94**, 220502 (2005).
[9] D. K. Serkland, M. M. Fejer, R. L. Byer, and Y. Yamamoto, Opt. Lett. **20**, 1649 (1995).
[10] M. E. Anderson, M. Beck, M. G. Raymer, and J. D. Bierlein, Opt. Lett. **20**, 620 (1995).
[11] G. S. Kanter, P. Kumar, R. V. Roussev, J. Kurz, K. R. Parameswaran, and M. J. Fejer, Opt. Express **10**, 177 (2002).
[12] L.-M. Duan, G. Giedke, J. I. Cirac, and P. Zoller, Phys. Rev. Lett. **84**, 2722 (2000).
[13] R. Simon, Phys. Rev. Lett. **84**, 2726 (2000).
[14] D. H. Jundt, Opt. Lett. **22**, 1553 (1997).
[15] M. Houé and P. D. Townsend, J. Phys. D **28**, 1747 (1995).
[16] N. Takei, N. Lee, D. Moriyama, J. S. Neergaard-Nielsen, and A. Furusawa, Phys. Rev. A **74**, 060101(R) (2006).